



Performance of silica-filled hybrid membranes dispersed by applying mediating surfactant in pervaporative removal of toluene from water

Iman Shams, Hamid Reza Mortaheb*

Chemistry and Chemical Engineering Research Center of Iran, Tehran 14335186, Iran, Tel. +98 21 88737853; email: St_Shams@ccerci.ac.ir (I. Shams), Tel. +98 21 44787751; Fax: +98 21 44787781; email: mortahab@ccerci.ac.ir (H.R. Mortaheb)

Received 1 October 2014; Accepted 18 January 2015

ABSTRACT

Novel hybrid membranes were prepared by dispersing silica nanoparticles in the active layer of the composite membrane using polyoxyethylene sorbitan monopalmitate (Tween 40) as the mediating surfactant. The fabricated membranes were characterized by Fourier transform infrared spectroscopy, wide-angle X-ray diffraction, thermal gravimetric analysis, scanning electron microscopy, energy-dispersive X-ray spectroscopy, optical contact angle, and swelling degree measurements. The pervaporative performances of these membranes for removal of toluene from mixtures with water were investigated in terms of mediating concentration. By increasing the mediating content in the membrane's matrix up to an optimum value of 2 wt.%, both toluene permeation flux and selectivity factor of the membrane were increased due to enhancement in the hydrophobicity and selective adsorption resulted from proper dispersion of the filler in the polymeric matrix. It was found that the membrane containing 2 wt.% mediating surfactant exhibits the highest selectivity factor of 7,779 and a permeation flux of $36.71 \text{ gm}^{-2}\text{h}$ for the feed with 150 ppm toluene at 25°C.

Keywords: Hybrid membrane; Silica nanoparticle; Mediating surfactant; Pervaporation; Volatile organic compounds

1. Introduction

Volatile organic compounds (VOCs) such as chlorinated and aromatic hydrocarbons including benzene, toluene, ethyl benzene, and xylene are of the most important pollutants in industrial wastewaters. These materials can be potentially considered as the pollutants of underground water resources. Due to growing concerns about their environmental impacts, restricting regulations are imposed on effluents of various industries.

Conventional methods such as distillation and liquid–liquid extraction are not economically feasible for purification of these low-concentration wastewaters [1,2]. Other cost-effective methods such as adsorption with activated carbon and air stripping are facing major problems e.g. requirement to regenerate the adsorbents or releasing pollutants from the aquatic environment into the air.

Applying pervaporation (PV) techniques for separation of different organic/organic and organic/aqueous mixtures has attracted many interests because of their high efficiencies [3,4]. In addition, PV can produce high-purity products from isomers, azeotropes,

*Corresponding author.

and close-boiling mixtures, which are hard to be separated by conventional methods. However, similar to other membrane techniques, PV suffers from the inherent drawback of trade-off effect between selectivity and permeability [5–9]. One effective solution is to use hybrid membranes [9–11], in which the matrix of organic polymer is filled with inorganic particles such as SiO_2 [12–14] and TiO_2 [15–17]. The hybrid membrane can benefit from the properties imparted by the inorganic fillers such as high selectivity, mechanical strength, and good thermal and chemical resistances as well as those of the polymeric matrix, i.e. simple processability and appropriate permeability. The hybrid membranes are also more cost effective than the ceramic membranes [18–23]. The most important characteristic of these hybrid membranes is to overcome the trade-off effect between the selectivity factor and permeation flux [8,24].

One of the most important problems in synthesis of nanoscale inorganic hybrids is aggregation of the fillers in the organic matrix that causes nonselective voids in the membrane's structure [25,26]. Many efforts such as grafting functional groups on the fillers [27–30], applying different kind of cross-linking agents [31,32], applying inorganic particles as precursors [30,33], *in situ* polymerization of monomers and inorganic precursors [34,35], and using other techniques have been performed recently for appropriate filler dispersion [13,36].

In this work, the filler agglomeration was controlled by introducing a mediating surfactant. Silica nanoparticles are chosen to fabricate the hybrid membrane with polydimethylsiloxane (PDMS) as the active layer supported on a polyethersulfone (PES) sublayer. Polyoxyethylene sorbitan monopalmitate (Tween 40) is used as the mediating surfactant. The silica content is kept constant at 10 wt.% according to the finding of Alizadeh Nourani et al. [37] and Beltran et al. [38], and the concentration of mediating surfactant is varied to improve the filler dispersion. The physical and spectroscopic properties of the fabricated membranes are investigated. The membranes are used for pervaporative separation of a toluene–water mixture at 25°C. The enhancement in the pervaporative performance of the membrane is then evaluated in terms of permeation flux, selectivity factor, and performance separation index.

2. Experimental

2.1. Materials

PDMS (viscosity = 5,000 MPa s and average molecular weight = 40,000), dibutyltin dilaurate (DBTL), and polyvinylpyrrolidone (PVP) (K90, $M_w = 360,000$) were

purchased from Sigma-Aldrich (USA). Polyethersulfone (Ultrason E6020 P, $M_w = 58,000$) was purchased from BASF. Silica nanoparticles with the purity of 99.9% and size of 10 nm were supplied by Nano Pars Lima (Iran). Tetraethyl orthosilicate (TEOS), Tween 40, toluene, and *n*-heptane were obtained from Merck (Germany). All reagents and chemicals were used as received without further purifications. Deionized water treated by a Millipore ultrapure water system was used in all the experiments.

2.2. Membrane preparation

In this study, flat-sheet-supporting layers of PES were prepared by dissolving PES and PVP with preset concentrations in dimethylacetamide using phase inversion technique. A detailed description about the preparation method of the supporting membrane was explained elsewhere [39].

In order to fabricate the top layer, PDMS, *n*-heptane, and silica nanoparticles were mixed together where the weight percent of silica on a solvent-free basis was set to the optimum value of 10% according to a previous research for the purpose of this study [37]. At the same time, a mixture of *n*-heptane and Tween 40 as the mediating surfactant with a ratio of 4:1 was prepared. Both solutions were stirred for 2 h on magnetic stirrers and were kept at 10°C. Required amounts of the surfactant solution were then added to the polymeric solution to adjust the mediating surfactant concentration. The prepared mixture was stirred for one more hour. Then, certain amounts of cross-linker TEOS and DBTL as the catalyst with a ratio of 0.02:0.1:1 (respect to PDMS) were added to the polymeric mixture. The suspension was then sonicated for 30 min and degassed under vacuum. The homogenized suspension was cast on the PES supporting layer as a thin film. The solvent in the top layer was then evaporated at room temperature, and thermally annealed in a vacuum oven at 75°C for 8 h.

The membranes were nominated based on the mediating content as M_0 , M_1 , M_2 , M_3 , and M_5 . For instance, M_0 is designated to the membrane without mediating surfactant, while M_5 is the membrane with 5 wt.% mediating surfactant on a solvent-free basis. All the membranes were stored in a dust-free and dry environment before being used in the PV experiments.

2.3. Membrane characterizations

2.3.1. Fourier transform infrared (FTIR) spectroscopy

FTIR spectra of the hybrid membranes were scanned (4,000–400 cm^{-1}) using a Bruker Tensor 27

FTIR spectrophotometer equipped with horizontal attenuated transmission accessories in the attenuated total reflectance mode.

2.3.2. Wide-angle X-ray diffraction

The morphologies of the hybrid membranes with various amounts of the surfactant were studied at room temperature using a Bruker's D8 advanced wide-angle X-ray diffractometer (Germany). The X-ray source was nickel-filtered Cu-K α radiation (40 kV, 30 mA). Dried membranes with uniform thicknesses of about 40 μm were mounted on a sample holder and the patterns were scanned in the reflection mode at 2θ angle of 4° – 70° with a rate of 8°C min^{-1} .

2.3.3. Thermal gravimetric analysis

The thermal stabilities of the PDMS hybrid membranes were examined by PerkinElmer TG/DTA thermogravimetric analyzer. The weights of samples were in the range of 5–8 mg. They were heated from ambient temperature to 800°C with a heating rate of $10^\circ\text{C min}^{-1}$ under a nitrogen stream with a flow rate of 25 mL min^{-1} to remove all possible corrosive gases. The intercept was taken as the glass transition temperature (T_g). Repeated runs after cooling with a rate of $10^\circ\text{C min}^{-1}$ exhibited reproducibility of T_g values within $\pm 1.5^\circ\text{C}$.

2.3.4. Scanning electron microscopy

The surface and cross-section morphologies of the hybrid membranes were observed by applying a JSM-840A scanning electron microscope (Zeiss Ultra 55, Germany) at 15 kV. All the samples were snapped in liquid nitrogen and coated with a 400 \AA conductive layer of sputtered gold. The weight percent of elements in the membrane structure was analyzed by EDAX (Sirius SD, e2v, UK).

2.3.5. Atomic force microscopy

The surface roughness of hybrid membranes was investigated by Atomic force microscopy (AFM). The AFM (DME Dual scope DS95–50–5E, Denmark) images were recorded on "height" and "phase" channels. Silicon cantilevers with pyramid tip (force constant = 0.07 – 0.4 Nm^{-1} , resonant frequency = 9 – 17 kHz) were used. The images were processed by the SPM program.

2.3.6. Optical contact angle (OCA) measurement

The contact angles of water on the hybrid membranes were measured using an OCA measurement

device (OCA-20, Data Physics, Germany). A water droplet with $5\text{-}\mu\text{L}$ volume was dropped on the membrane with a microsyringe in an air atmosphere. At least six contact angles at different locations on the surface of each membrane were measured and averaged.

2.3.7. Swelling degree (SD) of membrane

The SDs of membranes were determined using water–toluene mixtures with different compositions. The dry membranes were first soaked into the feed mixture in a sealed vessel at room temperature for 24 h. The swollen membranes were then wiped and quickly weighted on a digital microbalance (Mettler B204-S, Toledo, Switzerland) with an accuracy of $\pm 0.01\text{ mg}$. All the experiments were performed three times and the results were averaged. The percent of SD is calculated as:

$$\text{SD} = \frac{W_s - W_d}{W_d} \times 100 \quad (1)$$

where W_s and W_d are the weights of wet and dry membranes, respectively.

2.4. PV experiments

The schematic of applied setup in the PV experiments is shown in Fig. 1. The flat membrane is fixed on a ring module and placed between the two parts of a cylindrical PV cell. The whole cell is then packed by a set of rods, bolts, and ending supports. Effective area of membranes is 10 cm^2 . In order to minimize the effect of concentration polarization, the feed-side solution is stirred by a magnetic stirrer. The vacuum in the downstream side of the apparatus is maintained at

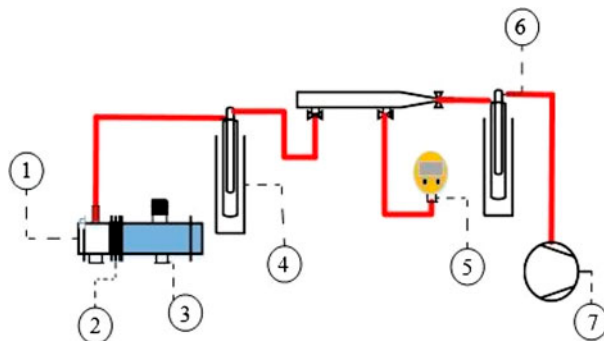


Fig. 1. Schematic of laboratory PV apparatus: (1) PV cell; (2) membrane module; (3) feed side; (4) cooling trap with nitrogen; (5) pressure indicator; (6) cooling trap; and (7) vacuum pump.

1 mbar using a two-stage vacuum pump (Edward, USA). The test membrane is allowed to be equilibrated in the feed compartment for about 1 h at 25°C before performing the PV experiment. The experiment is carried out for 5 h at 25°C and the permeate is collected in a cold trap, which is chilled by liquid nitrogen. The flux is calculated by weighing permeate on a digital microbalance with an accuracy of ± 0.01 mg. The samples are taken from the feed side at specified time intervals and their toluene concentrations are determined by UV–Vis technique (PerkinElmer, USA, $\lambda = 261.9$ nm). At least triple runs are performed for all the experiments and the results are averaged. The results of pervaporative experiments in this study were adequately reproducible.

The separation performances of the hybrid membrane can be assessed in terms of selectivity factor (α), permeation flux (J), PV separation index (PSI), and total normalized flux (J_n) as given in Table 1.

3. Results and discussion

3.1. Preparation and characterization of hybrid membranes

Due to hydrophilic nature of silica nanoparticles, uniform dispersion of these particles in the organic solvent is hard to be achieved by direct mixing.

Agglomeration of the particles in high concentrations restricts their usage.

Tween 40 as a polyoxyethylene derivative of sorbitan monolaurate is a stable and relatively nontoxic surfactant with wide applications in detergents. The hydrophile–lipophile balance (HLB) of Tween 40 is 15.6. The high HLB number of this surfactant will assist it to make proper bonds with aquatic and polar compounds [40].

During the synthesis of the hybrid membrane in this work, surfactant solution is added to the polymeric solution containing nanoparticles. The solution is homogenized under vigorous mechanical stirring. During this period, as shown in Fig. 2, the silica nanoparticles are placed among the polymeric network by aiding the surfactant. The spherical silica particles are embedded homogeneously within the PDMS matrix. Subsequently, crosslinking is completed by adding crosslinker and catalyst agents. The resulting hybrid membrane is then expected to be significantly different from that obtained by conventional methods such as solution blending.

3.2. Morphology and surface properties of hybrid composite membranes

Comparison of scanning electron microscopy (SEM) images in Fig. 3(a) and (b) reveals that when 2 wt.%

Table 1
Parameters used to evaluate PV performance

Selectivity factor (β)	$\alpha = \frac{Y_t/Y_w}{X_t/X_w} [-]$	Y_t and X_t : geometric means of toluene concentration in permeate and retentate, respectively. Subscripts “t” and “w” denote toluene and water, respectively
Permeation flux (J)	$J = \frac{M_p}{S_m \cdot t} [\text{g}(\text{m}^2 \text{h})^{-1}]$	M_p : weight of permeate (g) and S_m : surface area of membrane (m^2)
PV separation index (PSI)	$\text{PSI} = \alpha \times J [\text{g}(\text{m}^2 \text{h})^{-1}]$	
Total normalized flux (J_n)	$J_n = J \times l_m [\text{g}(\text{m h})^{-1}]$	l_m : membrane thickness (m)

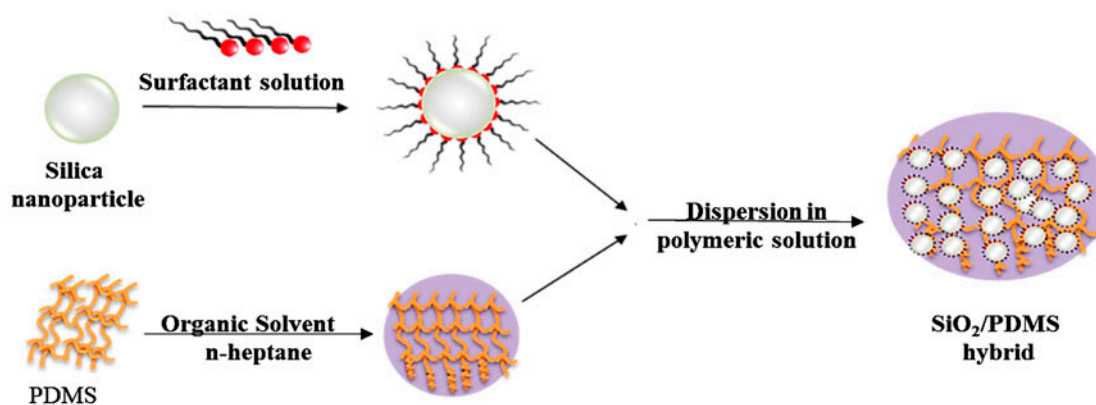


Fig. 2. Mechanism of functioning surfactant as mediating agent in fabricating hybrid membrane.

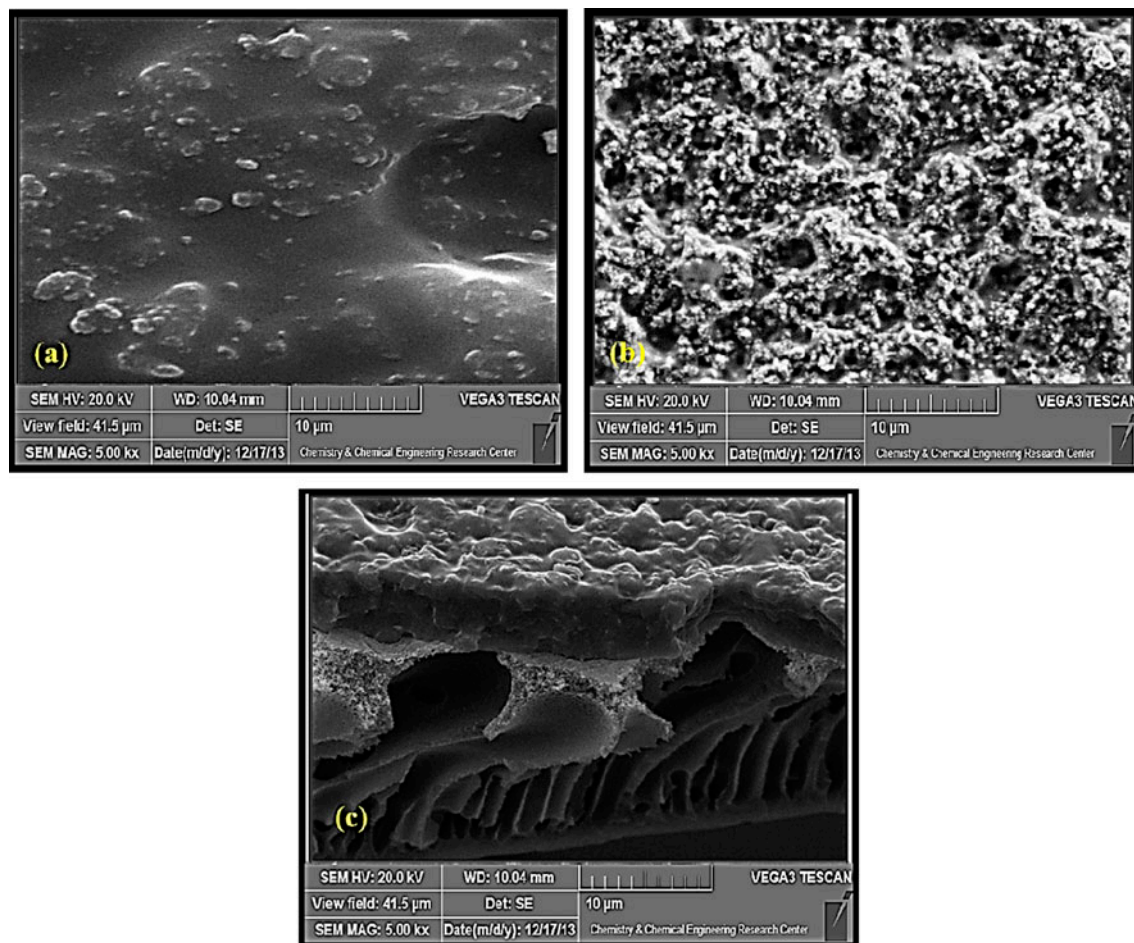


Fig. 3. SEM images of silica-filled hybrid membranes without surfactant (a), and with 2 wt.% surfactant: surface (b), cross-section (c); magnification of 5k \times .

mediating surfactant is applied (Fig. 3(b)), the dispersion of nanoparticle on the surface of hybrid membrane is completely different from that without applying mediating surfactant (Fig. 3(a)). Fig. 3(b) shows a perfect uniform dispersion of the particles, whereas some agglomerated particles and non-selective voids are noticeable in Fig. 3(a). The cross-sectional SEM image in Fig. 3(c) confirms the uniform dispersion of the particles in polymeric matrix of the membrane with 2 wt.% of surfactant.

The EDAX result for M_2 in Fig. 4 confirms that high amounts of Si exist on the surface of membrane having 2 wt.% surfactant.

AFM images of Fig. 5 show that the proper dispersion of filler particles in the membranes containing surfactant causes good roughness on the surface of those membranes in comparison with the surface of the membrane without surfactant. The roughness data including S_z (10 point height), S_a (arithmetic mean deviation), and S_q (root mean square deviation) in

Table 2 show the highest roughness for the membrane with 2 wt.% surfactant.

As seen in Fig. 6, the presence of excess surfactant in the polymeric solution at the higher contents (more

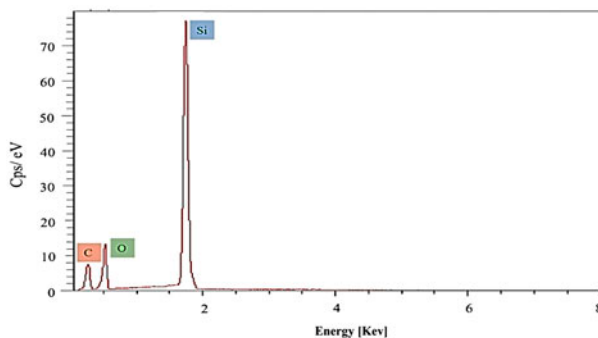


Fig. 4. EDAX curve of hybrid membrane having 2 wt.% surfactant (M_2).

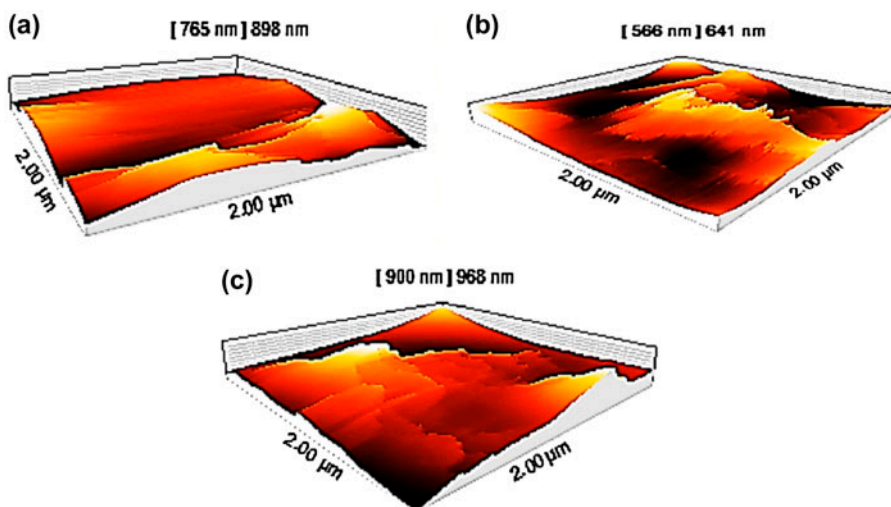


Fig. 5. AFM images of silica-filled hybrid membranes with 1 wt.% (a); 2 wt.% (b), and 5 wt.% (c) surfactant.

Table 2
Roughness parameters of membranes with various surfactant concentrations

Membrane	M_0	M_1	M_2	M_3	M_5
S_z (nm)	400	705	1,200	1,160	1,130
S_a (nm)	58	81	179	187	200
S_q (n)	97	109	238	240	252

than 2 wt.%) causes micelle formation [41], which not only may encapsulate the fillers but also results in void formation in the polymeric matrix as well as on

the membrane’s surface. The presence of free hydrophilic heads of the excess surfactant will tend to absorb more water which causes occupying active sites of fillers and deteriorates pervaporative performance of the corresponding membrane. The micelle formation is confirmed in the SEM image of M_5 (Fig. 7) with 5 wt.% surfactant.

The contact angles of membranes are presented in Fig. 8. The figure shows that the membrane with 2 wt.% surfactant has the highest hydrophobicity (contact angel = 147°). This result was expected since as found in SEM and AFM images, the membrane with 2 wt.% surfactant (M_2) has the highest roughness.

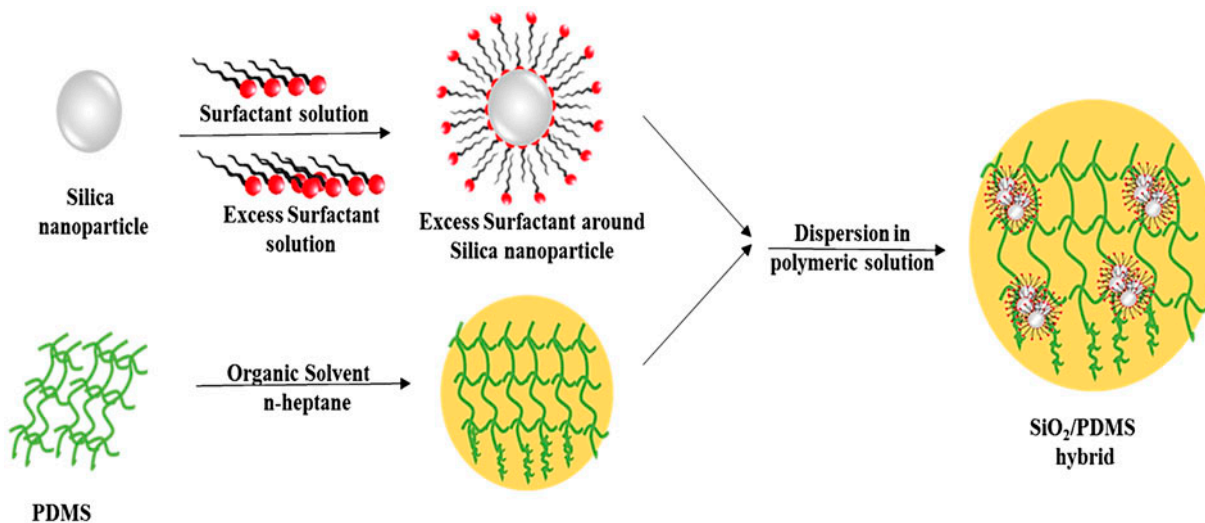


Fig. 6. Mechanism of micelle formation in presence of excess surfactant.



Fig. 7. SEM images of silica-filled hybrid membrane with 5 wt.% surfactant (Micelle formation around filler), magnification of 50k \times .

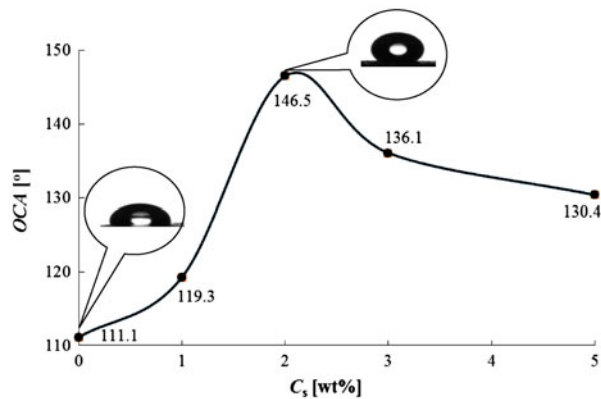


Fig. 8. Contact angles of hybrid membranes with various surfactant concentrations.

Based on the Wenzel correlation, the apparent contact angle is increased by the roughness of the surface in the case of a hydrophobic surface [42].

3.3. Physicochemical characterization of the flat-sheet films

FTIR spectra of the membranes without surfactant and with 2 and 5 wt.% surfactant in Fig. 9 confirm the presence of asymmetric Si–O–Si, symmetric Si–O–Si, Si–CH₃, and OH bands in the wavelength ranges of 1,000–1,150, 800–820, 1,200–1,300, and 2,800–3,600 cm⁻¹, respectively [43]. The intensities of each peak are similar because of the same filler content for all the membranes.

The X-ray diffraction spectra of hybrid membranes are shown in Fig. 10. The figure shows a broad peak between $2\theta = 12^\circ$ and 18° , which is corresponded to

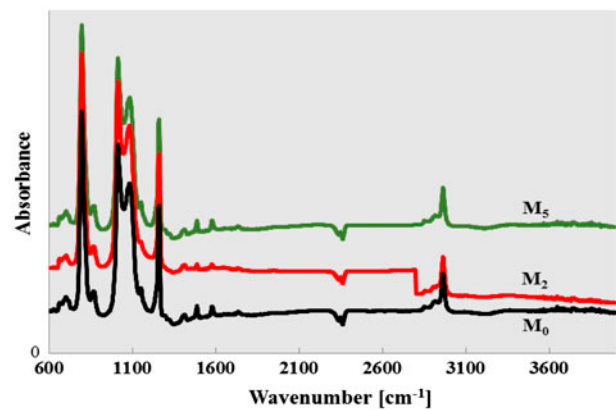


Fig. 9. FTIR spectra of hybrid membranes with different surfactant concentrations.

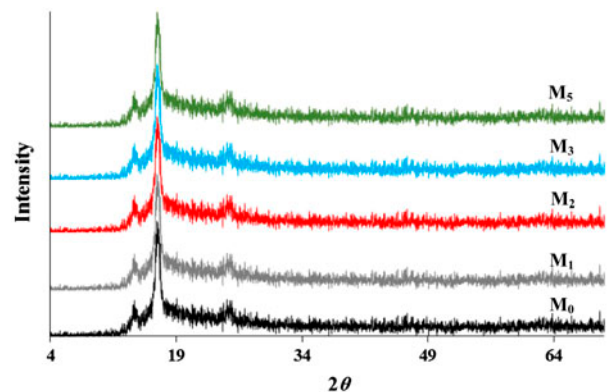


Fig. 10. XRD spectra of hybrid membranes with different surfactant concentrations.

the diffraction of PDMS segments [44,45] with similar intensities for all the membrane. The silica nanoparticles show a noisy pattern due to their amorphous structure with a broad peak between $2\theta = 10^\circ$ and 35° [37]. The peak of PDMS segments in the spectra of the composite membranes is partially covered by the silica spectrum.

The effect of filler dispersion on thermal stability of the membranes was evaluated by thermal gravimetric analysis tests. As shown in Fig. 11, the degradation temperature is increased for the membranes containing surfactant. This is directly related to the appropriate dispersion of the filler in the matrix that causes formation of proper bonds between the filler particles and the chains of the polymeric matrix. The proper filler dispersion also results in lower weight losses in the membranes containing surfactant in comparison to that without surfactant.

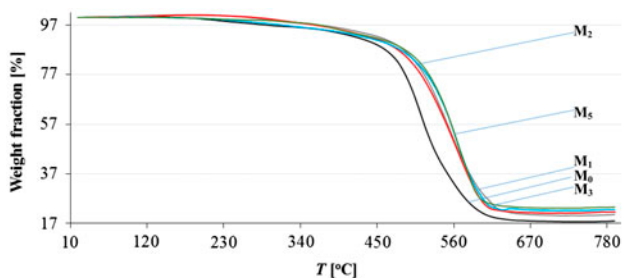


Fig. 11. Thermal gravimetric curves of hybrid membranes with different surfactant concentrations.

3.4. Pervaporation results

The pervaporative performances of the membranes are initially evaluated by measuring their SDs in the feeds with three different toluene concentrations of 12, 150, and 300 ppm. Fig. 12 shows that as expected SDs are increased by increasing toluene concentration in the feed for all the membranes because of high affinity of toluene toward PDMS [30,35,37,39,46]. However, for a certain feed concentration, the SD is reduced by increasing the surfactant concentration from 0 to 2 wt.% and it is then increased by further increase in the surfactant concentration. The decreased swellings of the membranes having up to 2 wt.% surfactant are related to uniform dispersion of the particles and proper bonding between the filler and the polymeric matrix, which prohibits from swelling. However, the excess free surfactant in the hybrid membranes (more than 2 wt.%) may lead to adsorption of more water due to the presence of free hydrophilic heads of the surfactant molecules and thus results in higher SDs.

This result is confirmed by considering the values of selectivity factor, α , in the pervaporative tests with

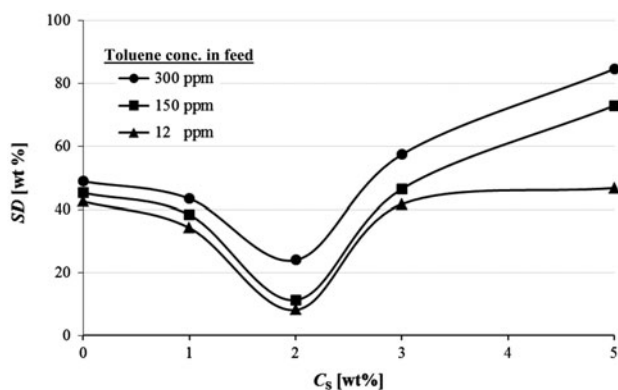


Fig. 12. Effect of surfactant content on SD of hybrid membranes in feeds with different toluene concentrations at 25°C.

the experimental setup as shown in Fig. 13. The figure shows that the selectivity factor increases by increasing surfactant content in the top layer of the tested membrane up to 2 wt.% and then it decreases. The selectivity factor of M_2 is 7,779, which is the highest value among the tested membranes. This can be attributed to the proper dispersion of the filler particles in the polymeric matrix. Meanwhile, all the membranes having mediating surfactant show higher selectivity factors than that of the membrane without surfactant.

Fig. 13 also represents PSI, of the tested hybrid membranes in the pervaporative experiments. Since PSI comprises both selectivity factor and permeation flux, it can be considered as a proper performance index. The figure confirms that M_2 has the optimum performance among the tested membranes.

Fig. 14 shows total, toluene, and water permeation fluxes in the pervaporative experiments. Again,

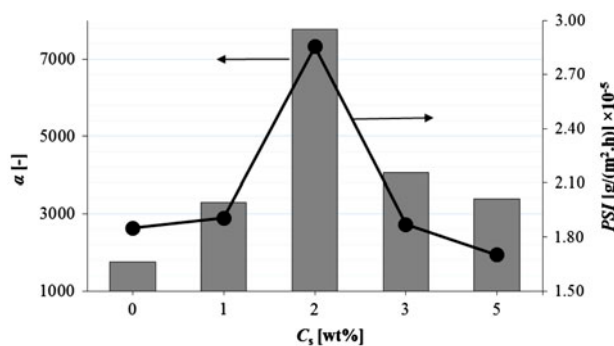


Fig. 13. Effect of mediating surfactant on selectivity factor and PSI in pervaporative experiments of hybrid membranes; feed temperature = 25°C, feed concentration = 150 ppm.

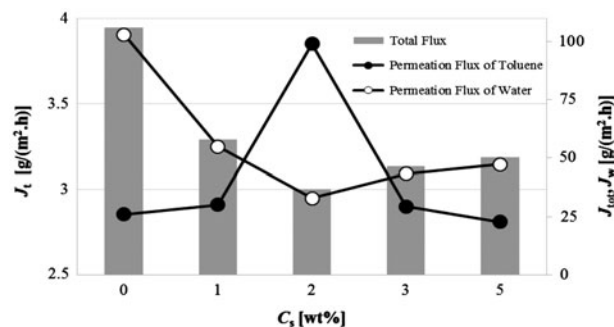


Fig. 14. Effect of mediating surfactant on total, toluene, and water permeation fluxes in pervaporative experiments; feed temperature = 25°C, feed concentration = 150 ppm.

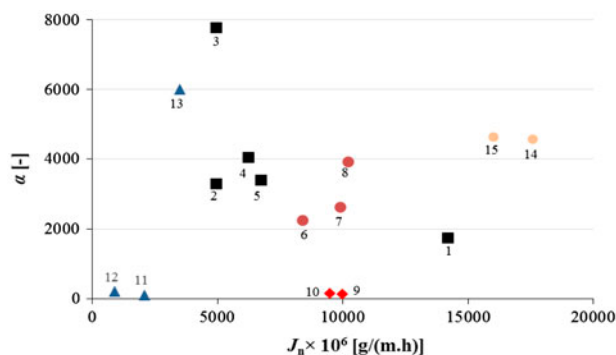


Fig. 15. Performance of modified PDMS membranes applied for pervaporative removal of VOCs from water.

(1) M_0 ; (2) M_1 ; (3) M_2 ; (4) M_3 ; (5) M_5 ; (6) filled PDMS with SiO₂ 10 nm [37]; (7) filled PDMS with SiO₂ 80 nm [37]; (8) filled PDMS with Silicalite-1 [37]; (9) filled PDMS with unmodified Silicalite-1 [30]; (10) filled PDMS with modified Silicalite-1 [30]; (11) unfilled PDMS/PAN [45]; (12) filled PDMS with CB/PAN [45]; (13) filled PDMS with CB [45]; (14) filled PDMS with C-Calix Arene [46]; (15) filled PDMS with Calix Arene derivatives [46].

toluene permeation flux is increased by increasing surfactant concentrations up to 2 wt.% while water permeation flux shows a reverse tendency. The performance of the membranes having more than 2 wt.% surfactant is deteriorated partially due to the effect of micelle formation and decrease in permselectivity.

In order to compare the performances of the prepared membranes in this research and those from previous studies for removal of VOCs from water, the corresponded selectivity factors and total normalized fluxes are illustrated in Fig. 15. The figure shows that the membrane containing silica nanoparticles in presence of 2 wt.% mediating surfactant represents the most feasible performance that is the highest separation factor as well as an adequate permeation flux.

4. Conclusion

In this research, Tween 40 was incorporated as a mediating surfactant in fabrication of hybrid membranes comprised of a dense PDMS top layer filled with silica nanoparticles supported on a porous PES sublayer. The fabricated membranes were characterized and then tested in pervaporative tests by an experimental setup for removal of toluene from water. It was found that the surfactant with concentrations up to 2 wt.% significantly helps the filler to be uniformly dispersed in the top layer of the membrane, so that the membrane having 2 wt.% surfactant exhibits the best performance for pervaporative separation of a

150 ppm feed, i.e. selectivity factor of 7,779, permeation flux of 36.71 gm⁻²h, and PSI of 285,540 gm⁻²h. However, excessive surfactant may depreciate the performance of the membrane due to micelle formation, which tends to deteriorate the uniformity of filler dispersion and arrangement of polymer chains causing unselective interfacial voids and adsorption of higher amounts of water.

Acknowledgments

This work was supported by Iran Nanotechnology initiative council. The authors would like to thank Dr Reza Zadmand for his supportive consultations.

References

- [1] F. Lipnizki, R.W. Field, P.K. Ten, Pervaporation-based hybrid process: A review of process design, applications and economics, *J. Membr. Sci.* 153 (1999) 183–210.
- [2] F. Lipnizki, S. Hausmanns, P.K. Ten, R.W. Field, G. Laufenberg, Organophilic pervaporation: Prospects and performance, *Chem. Eng. J.* 73 (1999) 113–129.
- [3] A. Jonquieres, R. Clement, P. Lochon, J. Néel, M. Dresch, B. Chrétien, Industrial state-of-the-art of pervaporation and vapour permeation in the western countries, *J. Membr. Sci.* 206 (2007) 87–117.
- [4] V. Van Hoof, L. Van den Abeele, A. Buekenhoudt, C. Dotremont, R. Leysen, Economic comparison between azeotropic distillation and different hybrid systems combining distillation with pervaporation for the dehydration of isopropanol, *Sep. Purif. Technol.* 37 (2004) 33–49.
- [5] A. Kittur, S. Kulkarni, M. Aralaguppi, M. Kariduraganavar, Preparation and characterization of novel pervaporation membranes for the separation of water-isopropanol mixtures using chitosan and NaY zeolite, *J. Membr. Sci.* 247 (2005) 75–86.
- [6] C.L. Li, S.H. Huang, W.S. Hung, S.T. Kao, D.M. Wang, Y. Jean, K.R. Lee, J.Y. Lai, Study on the influence of the free volume of hybrid membrane on pervaporation performance by positron annihilation spectroscopy, *J. Membr. Sci.* 313 (2008) 68–74.
- [7] S.J. Lue, S. Peng, Polyurethane (PU) membrane preparation with and without hydroxypropyl- β -cyclodextrin and their pervaporation characteristics, *J. Membr. Sci.* 222 (2003) 203–217.
- [8] F. Peng, L. Lu, H. Sun, Y. Wang, J. Liu, Z. Jiang, Hybrid organic-inorganic membrane: Solving the tradeoff between permeability and selectivity, *Chem. Mater.* 17 (2005) 6790–6796.
- [9] R. Qi, Y. Wang, J. Chen, J. Li, S. Zhu, Pervaporative desulfurization of model gasoline with Ag₂O filled PDMS membranes, *Sep. Purif. Technol.* 57 (2007) 170–175.
- [10] S.S. Kulkarni, A.A. Kittur, M.I. Aralaguppi, M.Y. Kariduraganavar, Synthesis and characterization of hybrid membranes using poly (vinyl alcohol) and tetraethylorthosilicate for the pervaporation separation of water-isopropanol mixtures, *J. Appl. Polym. Sci.* 94 (2004) 1304–1315.

- [11] L. Lin, Y. Zhang, H. Li, Pervaporation and sorption behavior of zeolite-filled polyethylene glycol hybrid membranes for the removal of thiophene species, *J. Colloid Interface Sci.* 350 (2010) 355–360.
- [12] B. Li, W. Liu, H. Wu, S. Yu, R. Cao, Z. Jiang, Desulfurization of model gasoline by bioinspired oleophilic nanocomposite membranes, *J. Membr. Sci.* 415 (2012) 278–287.
- [13] B. Li, S. Yu, Z. Jiang, W. Liu, R. Cao, H. Wu, Efficient desulfurization by polymer-inorganic nanocomposite membranes fabricated in reverse microemulsion, *J. Hazard. Mater.* 211 (2012) 296–303.
- [14] S. Yi, Y. Su, B. Qi, Z. Su, Y. Wan, Application of response surface methodology and central composite rotatable design in optimizing the preparation conditions of vinyltriethoxysilane modified silicalite/polydimethylsiloxane hybrid pervaporation membranes, *Sep. Purif. Technol.* 71 (2010) 252–262.
- [15] W. Liu, B. Li, R. Cao, Z. Jiang, S. Yu, G. Liu, H. Wu, Enhanced pervaporation performance of poly (dimethyl siloxane) membrane by incorporating titania microspheres with high silver ion loading, *J. Membr. Sci.* 378 (2011) 382–392.
- [16] M. Sairam, M.B. Patil, R.S. Veerapur, S.A. Patil, T.M. Aminabhavi, Novel dense poly (vinyl alcohol)-TiO₂ mixed matrix membranes for pervaporation separation of water-isopropanol mixtures at 30°C, *J. Membr. Sci.* 281 (2006) 95–102.
- [17] T. Zhu, Y. Lin, Y. Luo, X. Hu, W. Lin, P. Yu, C. Huang, Preparation and characterization of TiO₂-regenerated cellulose inorganic-polymer hybrid membranes for dehydration of caprolactam, *Carbohydr. Polym.* 87 (2012) 901–909.
- [18] P.C. Chiang, W.T. Whang, M.H. Tsai, S.C. Wu, Physical and mechanical properties of polyimide/titania hybrid films, *Thin Solid Films* 447 (2004) 359–364.
- [19] G. Clarizia, C. Algieri, E. Drioli, Filler-polymer combination: A route to modify gas transport properties of a polymeric membrane, *Polymer* 45 (2004) 5671–5681.
- [20] C. Guizard, A. Bac, M. Barboiu, N. Hovnanian, Hybrid organic-inorganic membranes with specific transport properties: Applications in separation and sensors technologies, *Sep. Purif. Technol.* 25 (2001) 167–180.
- [21] Z. Lu, G. Liu, S. Duncan, Poly (2-hydroxyethyl acrylate-co-methyl acrylate)/SiO₂/TiO₂ hybrid membranes, *J. Membr. Sci.* 221 (2003) 113–122.
- [22] A. Taniguchi, M. Cakmak, The suppression of strain induced crystallization in PET through sub micron TiO₂ particle incorporation, *Polymer* 45 (2004) 6647–6654.
- [23] Y. Yang, P. Wang, Preparation and characterizations of a new PS/TiO₂ hybrid membranes by sol-gel process, *Polymer* 47 (2006) 2683–2688.
- [24] F. Peng, L. Lu, H. Sun, Y. Wang, H. Wu, Z. Jiang, Correlations between free volume characteristics and pervaporation permeability of novel PVA-GPTMS hybrid membranes, *J. Membr. Sci.* 275 (2006) 97–104.
- [25] T.T. Moore, W.J. Koros, Non-ideal effects in organic-inorganic materials for gas separation membranes, *J. Mol. Struct.* 739 (2005) 87–98.
- [26] T.T. Moore, R. Mahajan, D.Q. Vu, W.J. Koros, Hybrid membrane materials comprising organic polymers with rigid dispersed phases, *AIChE J.* 50 (2004) 311–321.
- [27] P.N. Patel, J.M. Zielinski, J. Samseth, R.J. Spontak, Effects of pressure and nanoparticle functionality on CO₂-selective nanocomposites derived from cross-linked poly (ethylene glycol), *Macromol. Chem. Phys.* 205 (2004) 2409–2419.
- [28] D. Shekhawat, D.R. Luebke, H.W. Pennline, A Review of Carbon Dioxide Selective Membranes: A Topical Report. Office of Scientific and Technical Information (OSTI), US Department of Energy, Morgantown, WV, 2003.
- [29] P. Studer, V. Larras, G. Riess, Amino end-functionalized poly(ethylene oxide)-block-poly(methylidene malonate 2.1.2) block copolymers: Synthesis, characterization, and chemical modification for targeting purposes, *Eur. Polym. J.* 44 (2008) 1714–1721.
- [30] H. Zhou, Y. Su, X. Chen, S. Yi, Y. Wan, Modification of silicalite-1 by vinyltrimethoxysilane (VTMS) and preparation of silicalite-1 filled polydimethylsiloxane (PDMS) hybrid pervaporation membranes, *Sep. Purif. Technol.* 75 (2010) 286–294.
- [31] L. Lin, Y. Kong, G. Wang, H. Qu, J. Yang, D. Shi, Selection and crosslinking modification of membrane material for FCC gasoline desulfurization, *J. Membr. Sci.* 285 (2006) 144–151.
- [32] X. Zhan, J.D. Li, J.Q. Huang, C.X. Chen, Pervaporation properties of PDMS membranes cured with different cross-linking reagents for ethanol concentration from aqueous solutions, *Chin. J. Polym. Sci.* 27 (2009) 533–542.
- [33] L.K. Pandey, C. Saxena, V. Dubey, Modification of poly (vinyl alcohol) membranes for pervaporative separation of benzene/cyclohexane mixtures, *J. Membr. Sci.* 227 (2003) 173–182.
- [34] L. Nicolais, G. Carotenuto, *Metal-Polymer Nanocomposites*, John Wiley & Sons, Hoboken, NJ, 2004.
- [35] Q.L. Liu, J. Xiao, Silicalite-filled poly (siloxane imide) membranes for removal of VOCs from water by pervaporation, *J. Membr. Sci.* 230 (2004) 121–129.
- [36] Z.L. Xu, L.Y. Yu, L.F. Han, Polymer-nanoinorganic particles composite membranes: A brief overview, *Front. Chem. Eng. Chin.* 3 (2009) 318–329.
- [37] E. Alizadeh Nourani, H.R. Mortaheb, M.R. Ehsani, Pervaporative performances of mixed matrix membranes filled with silica/silicalite-1 particles for purification of toluene from dilute aqueous solution, *J. Environ. Chem. Eng.* 2 (2014) 888–898.
- [38] A.B. Beltran, G.M. Nisola, S.S. Choi, Y. Kim, W.J. Chung, Surface-functionalized silica nanoparticles as fillers in polydimethylsiloxane membrane for the pervaporative recovery of 1-butanol from aqueous solution, *J. Chem. Technol. Biotechnol.* 88 (2013) 2216–2226.
- [39] S.S. Shahrabi, H.R. Mortaheb, J. Barzin, M.R. Ehsani, Pervaporative performance of a PDMS/blended PES composite membrane for removal of toluene from water, *Desalination* 287 (2012) 281–289.
- [40] V. Polychniatou, C. Tzia, Study of formulation and stability of co-surfactant free water-in-olive oil nano and submicron emulsions with food grade non-ionic surfactants, *J. Am. Oil Chem. Soc.* 91 (2014) 79–88.
- [41] S. Mandal, C. Banerjee, S. Ghosh, J. Kuchlyan, N. Sarkar, Modulation of the photophysical properties of curcumin in non-ionic surfactant (Tween-20) forming micelles and niosomes: A comparative study of different microenvironments, *J. Phys. Chem. B* 117 (2013) 6957–6968.

- [42] D. Quéré, Wetting and roughness. *Annu. Rev. Mater. Res.* 38 (2008) 71–99.
- [43] B.Shokri, M.A. Firouzjah, S. Hosseini, FTIR Analysis of Silicon Dioxide Thin Film Deposited by Metal Organic-based PECVD, ISPC19-2009, Bochum, Germany.
- [44] J.H. Kim, Y.M. Lee, Gas permeation properties of poly (amide-6-b-ethylene oxide)–silica hybrid membranes, *J. Membr. Sci.* 193 (2001) 209–225.
- [45] L. Liu, Z. Jiang, F. Pan, F. Peng, H. Wu, The unusual change of permeation rate in PDMS membranes filled with crystalline calixarene and its derivative, *J. Membr. Sci.* 279 (2006) 111–119.
- [46] D. Panek, K. Konieczny, Preparation and applying the membranes with carbon black to pervaporation of toluene from the diluted aqueous solutions, *Sep. Purif. Technol.* 57 (2007) 507–512.